Chapter 6

Electrostimulation On Conducting Surface Initiate Rapid Neurogenic Differentiation of hMSCs

6.1 Introduction

The presence of indigenous electric properties in nerve tissues has paved the way to use electrical stimulations to promote neuronal differentiation, guided cell migration, alignment, neurite outgrowth and synapse formation [278-282]. The use of electric stimulations in the form of alternating, direct, pulse, monophasic and biphasic currents has been investigated to direct stem cell differentiation into neurons. Electric stimulations to the cells have been applied through direct, capacitive, inductive, or combined electrical coupling to achieve lineage-specific differentiation [283,284]. The effect of different frequency ranges of electromagnetic fields, voltage, and stimulation duration have been established as crucial parameters to generate different responses to direct neuronal differentiation of stem cell populations [285,286]. These studies infer that types of electrical stimulation and their delivery method play a crucial role in defining the differentiation process. The strategies adopted in the past for transference of electric stimulation showed promising results, but most of them employed a long duration of stimulation with repetition and required replacement with fresh culture media at every time of stimulation [287-291]. These methods could present multiple challenges, including maintaining contamination-free cell growth conditions, retaining high cell viability, and ensuring homogenous stimulation.

This study describes a method to provide one-time electrical stimulation of short duration (< 200 s) to hMSCs adherent on indium tin oxide (ITO) through a potentiostat in culture media to induce neurogenic differentiation. The defined method offers advantages of rapid differentiation, scalability with a high degree of reproducibility and retaining cell viability

without changing media. The effect of electrostimulation on mitochondrial membrane potential (MMP, $\Delta\Psi_M$) and corresponding initiation of reactive oxygen species (ROS) production were investigated.

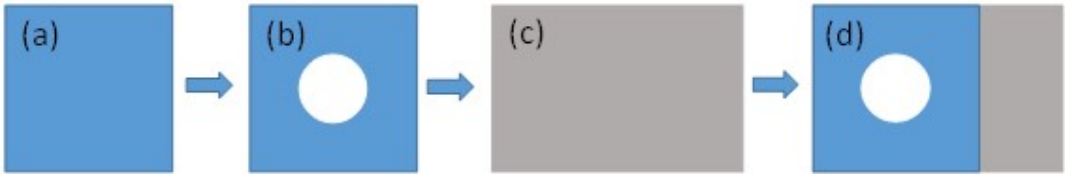

Figure 6.1: Schematic representation of the process of fabrication of cell culturing platform. (a) PDMS film, (b) PDMS films having micro-machined through physical patterning, (c) ITO surface, and (d) adhesion of ITO with PDMS.

6.2 Fabrication of cell culturing platform

A schematic diagram in **Figure 6.1** shows different steps used to fabricate a cell culturing platform to provide electrostimulation to cells. In this, thin sheets (~8 mm) of PDMS were prepared by casting its degassed solution (base and curing agent in the ratio of 10:1) in a mold kept at 45°C for 24 h. These sheets were cut into 1 cm × 1 cm, then a hole in the center was created using a punching system. The ITO glass plate was also carved into a rectangular shape of 1 cm × 1.5 cm. The PDMS sheet having a hole was gently placed at one edge of ITO and pressed to achieve air-tight sealing. This assembly of PDMS sheet on ITO substrate created a well-like structure having conducting surface of ITO as its base. The fabricated platforms were placed in a cell culture dish and sterilized with UV light for 15 min, prior to cell seeding. hMSCs were cultured in stem cell complete growth media at 37°C in a humidified atmosphere containing 5% CO_2 and routinely observed under an inverted microscope for contamination. The medium was replaced every 2 or 3 days and trypsinized until cell growth achieved 80-90% confluency. hMSCs were seeded at a density of 3×10^3 in the well of the fabricated

platform and incubated for 24 h before further experimentation to allow the cells to attain their typical morphological characteristics. **Figure 6.2** shows a microscopic image of cells inside the physical patterned surface.

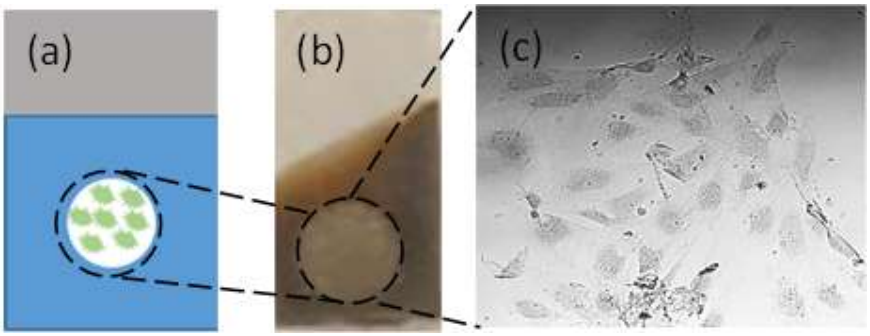

Figure 6.2: (a) Schematic representation of cell culturing platform, (b) optical image of cell culturing platform with cells, and (c) microscopic image of cells.

6.3 Electrical stimulation to hMSCs

The cell culturing platform was used for growing hMSC and providing them the selective biasing to study the effect of electrostimulations on conducting surfaces. **Figure 6.3** shows a schematic representation of the experimental set-up for this. To provide selective biasing, a conventional three-electrode setup was used to provide voltage biasing to the cells. The hMSCs laden platform was used as a working electrode connected to the potentiostat with platinum wire as a counter electrode and saturated calomel as the reference electrode. Then the cells were stimulated with different voltage biasing at variable scan rates to optimize the appropriate conditions.

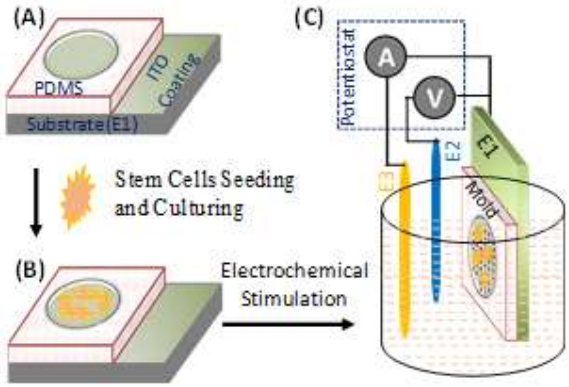

Figure 6.3: Process of providing electrostimulation to hMSCs. Schematic representation of (A) cell culturing platform, (B) seeding of hMSCs into the fabricated well, and (C) voltage biasing and the I-V measuring system.

The schematic representation in **Figure 6.3** shows the fabrication of the working electrode (E1), hMSCs adherent to ITO, and connecting it to a reference electrode (E2) which does not allow current to flow across the WE and RE while applying different voltage biases across them in the culture media. Thus, applying various voltage biases on the E1 can modulate the rate of ion transport through the adherent hMSCs into culture media, which was measured by placing a counter electrode (E3).

One-time potential biasing (at variously biasing ranges as ± 0.5 V, ± 1.0 V, and ± 1.5 V) was applied to adherent hMSCs on the conducting surface placed inside the culture media. The current-voltage response of the electrode E1 was measured at these three different potentials biasing provided inside the culture media and it was recorded. The results are shown in **Figure 6.4**. The effect of these biases on hMSCs could significantly affect the influx of ions into the cellular compartment and the oxidation and reduction of cellular redox molecules. The current-voltage response for a complete cycle starting from negative to positive and then reverse does not show any significant hysteresis in the positive biasing (forward region) for ±

0. 5 V and ± 1 V, whereas only a small hysteresis effect in the current was observed in the negative biasing (reverse region).

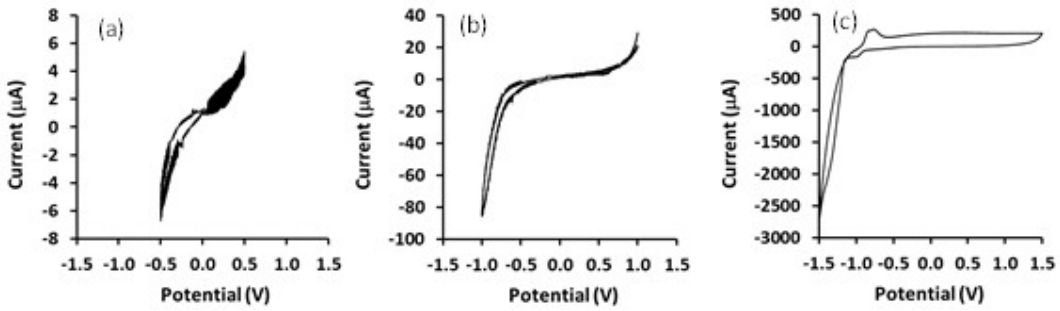

Figure 6.4: Current-Voltage response during electrical stimulation inside the culture media (a) ± 0.5 V, (F) ± 1.0 V and (G) ± 1.5 V.

The biasing potential in the range from - 1.5 V to + 1.5 V had shown a rapid increase in both positive and negative current along with the hysteresis effect. The current-voltage response also showed distinct peaks between -0.6 V to -0.9 V for a positive current and from -0.9 V and -1.1 V for a negative current. No specific peaks were observed in the current-voltage response associated with only cell culture media. Similarly, the working electrode E1, containing adherent hMSCs, did not also show such a peak at the potential bias at relatively lower biasing potential in the range of ± 0.5 V and ± 1.0 V in the cyclic response.

Further, the cells that received electrostimulation at various conditions and unstimulated cells (described as control), adherent on the conducting surface, were further incubated for 24 h in a fresh culture media. Cell viability was evaluated by performing the dual staining with Hoechst 33342/and PI that pictures simultaneous fluorescence of viable and dead cells. Hoechst 33342, a cell-permeable dye, stains the total cell populations while PI cannot pass through a viable cell membrane. It reaches the nucleus by diffusing through the comprised membrane of dead cells and intercalating with their DNA to emit red fluorescence, thus

staining non-viable cells. After twenty-four hours of stimulation, the depleted media was aspirated from the culture dish, and cell adherent platforms were washed thoroughly with PBS. The stimulated and control

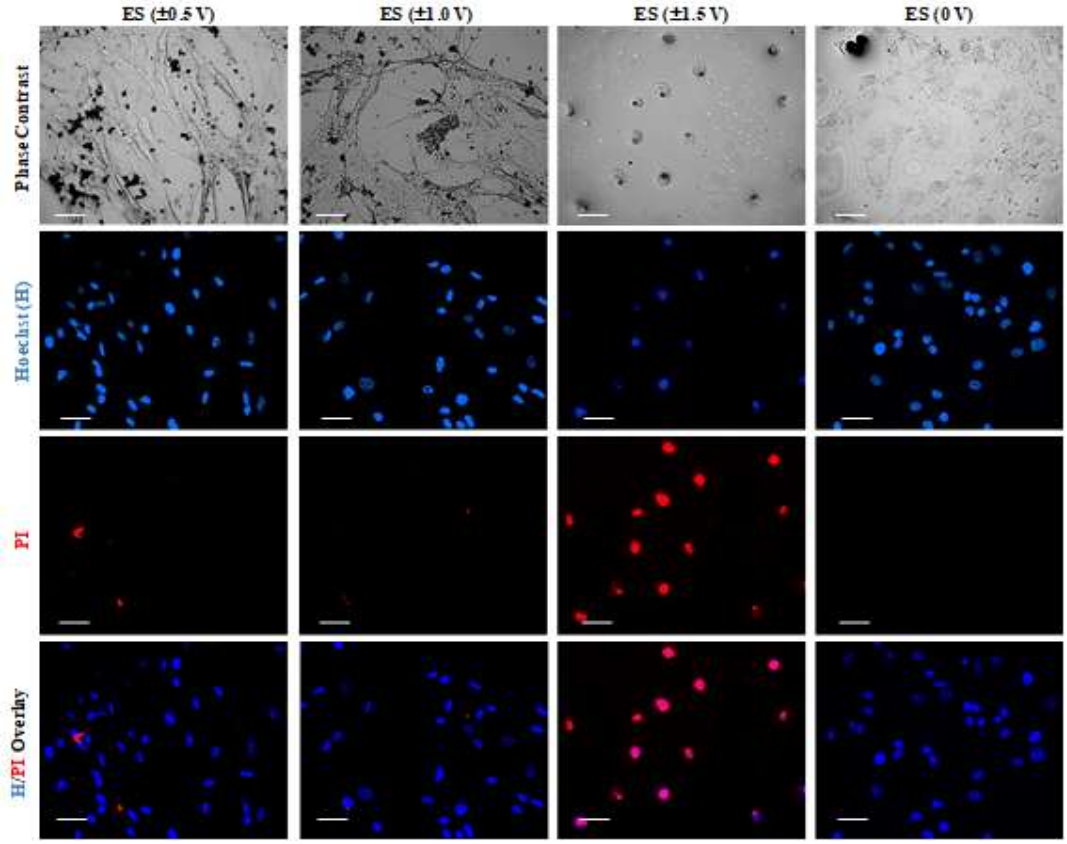

Figure 6.5: Phase-contrast images along with Hoechst 33342/PI dual staining of adherent hMSCs after 24 h of receiving electrical stimulations. The ES (0 V) corresponds to hMSCs that did not receive electrical stimulation. Scale bar 100 μM.

hMSCs were successfully stained with a solution of Hoechst 33342 (1 μg mL^{-1}) and PI (1 μg mL^{-1}) and incubated for 30 min at 37°C in the dark. The cells were finally washed with PBS before examining under an inverted fluorescence microscope. The results are shown in **Figure 6.5** with phase-contrast images. A voltage bias of ± 0.5 V and ± 1.0 V did not showed any red-stained cell population. In comparison, cells stimulated with ± 1.5 V showed an upsurge in dead cells, confirming the inactivation of a larger population of cells. This could be due to

irreversible oxidation and reduction of redox molecules present within the cellular system, as observed in Figure 1G. The hMSCs on ITO without losing their viability after receiving one bias of ± 0.5 V and ± 1.0 V are described as electrostimulated (ES) and adherent hMSCs on the ITO surface without

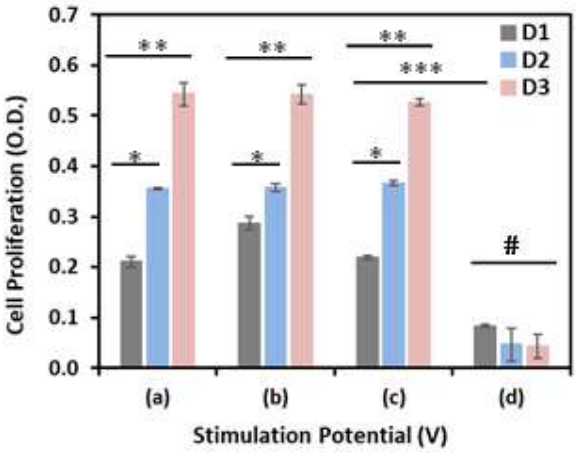

*Figure 6.6: Cell proliferation of hMSCs at day 1 (D1), day 2 (D2), and day 3 (D3). (a) hMSCs and (b-d) electrostimulated ((b) ±0.5 V, (c) ± 1.0 V, (d) ± 1.5 V) hMSCs. #, *, ** and *** represent P < 0.05 for n = 36 ITO substrates in the experiments.*

biasing (± 0.0 V) is defined as unstimulated (US) for further quantifying the effect of stimulation in their state by culturing them for different days. The cell proliferation of stimulated and unstimulated hMSCs was assessed at day 1 (D1), day 2 (D2), and day 3 (D3). MTT assay was used to quantify the metabolic activity of viable cells in a time-dependent manner by recording changes in absorbance of formazan crystal at 570 nm using a plate reading spectrophotometer. At different specified time intervals, MTT solution (0.2 mg/ml) in culture medium was added and incubated for 4 h at 37°C. After the incubation, the MTT solution was discarded and replaced with dimethyl sulfoxide (DMSO, HiMedia) to dissolve the formed formazan crystals. After 30 min, absorbance was taken by a microplate reader (Synergy H1 hybrid, Biotek, USA) and the results were expressed as cell concentration. In each experiment, n =3 platforms were used, and each experiment was repeated three times.

The results of cell proliferation are shown in **Figure 6.6**. The finding confirms a comparable cell proliferation rate for the control and cells that received stimulation with relatively less bias potential in the range of -0.5 V to + 0.5 V and - 1.0 V to + 1.0 V. However, the potential bias at the higher range of potential from - 1.5 V to + 1.5 V made the cells becomes nonproliferable.

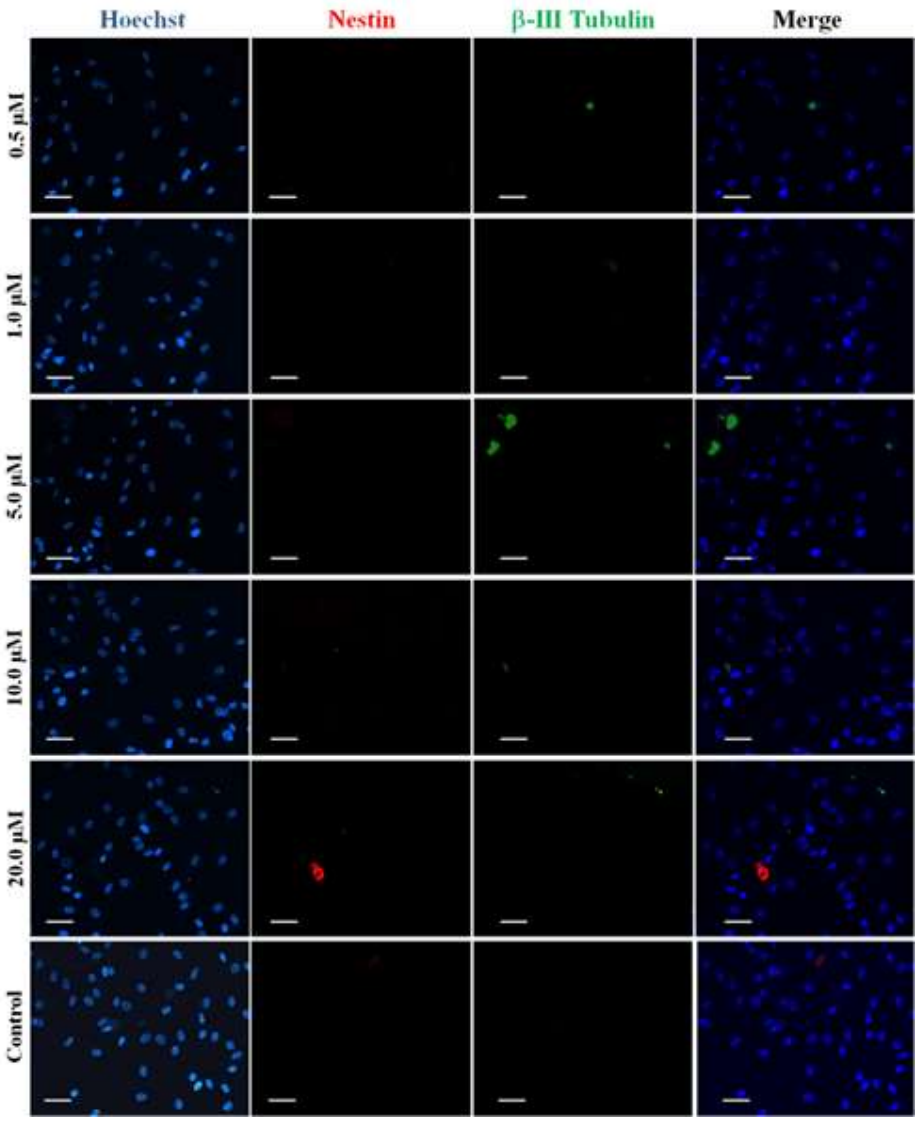

Figure 6.7: Shows image of different staining (Hoechst, Nestin, β-III Tubulin and merge) of adherent hMSCs on ITO surface cultured in different concentrations of retinoic acid (0.5 µM, 1.0 µM, 5.0 µM, 10.0 µM, 20.0 µM and control condition (0.1% DMSO)) after day 1 of the culture.

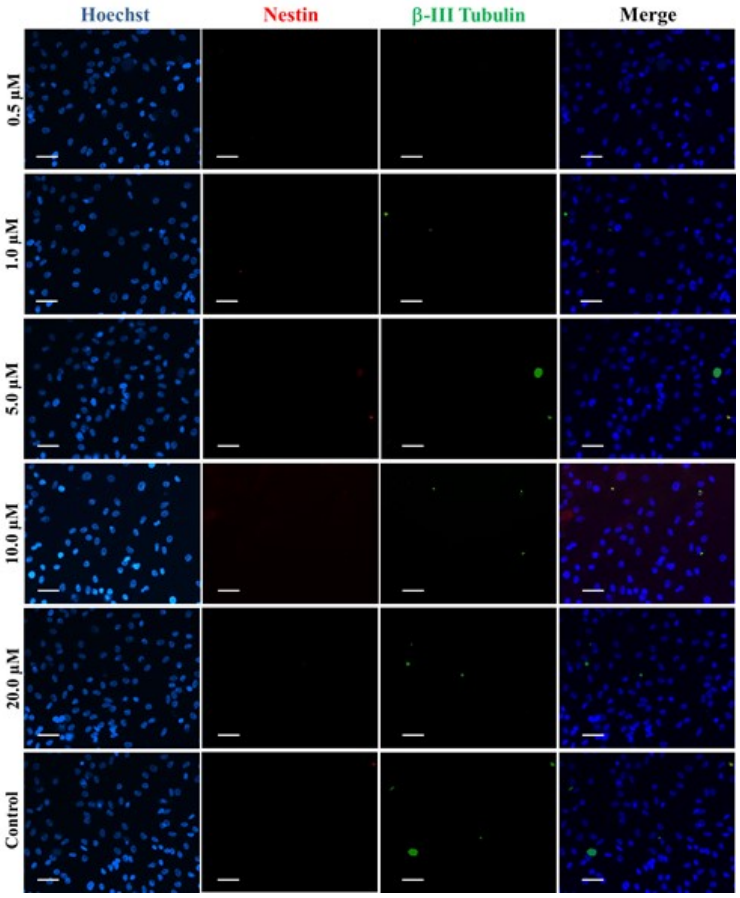

Figure 6.8: Shows image of different staining (Hoechst, Nestin, β-III Tubulin and merge) of adherent hMSCs on ITO surface cultured in different concentrations of retinoic acid (0.5 µM, 1.0 µM, 5.0 µM, 10.0 µM, 20.0 µM and control condition (0.1% DMSO)) after day 3 of the culture.

6.4 Retinoic acid stimulation to hMSCs

Retinoic acid is well known for its capability for inducing neurogenic differentiation of the stem cell. Previously the effect of retinoic acid (RA) stimuli has been used to prompt neurodifferentiation of human stem cells and their proliferation [292-294]. Thus, it will provide the standard conditions required for achieving selective differentiation of stem cells into neurons with the required the concentration of retinoic acid and the expected time it takes to initiate the differentiation process. These control conditions will be used to compare the

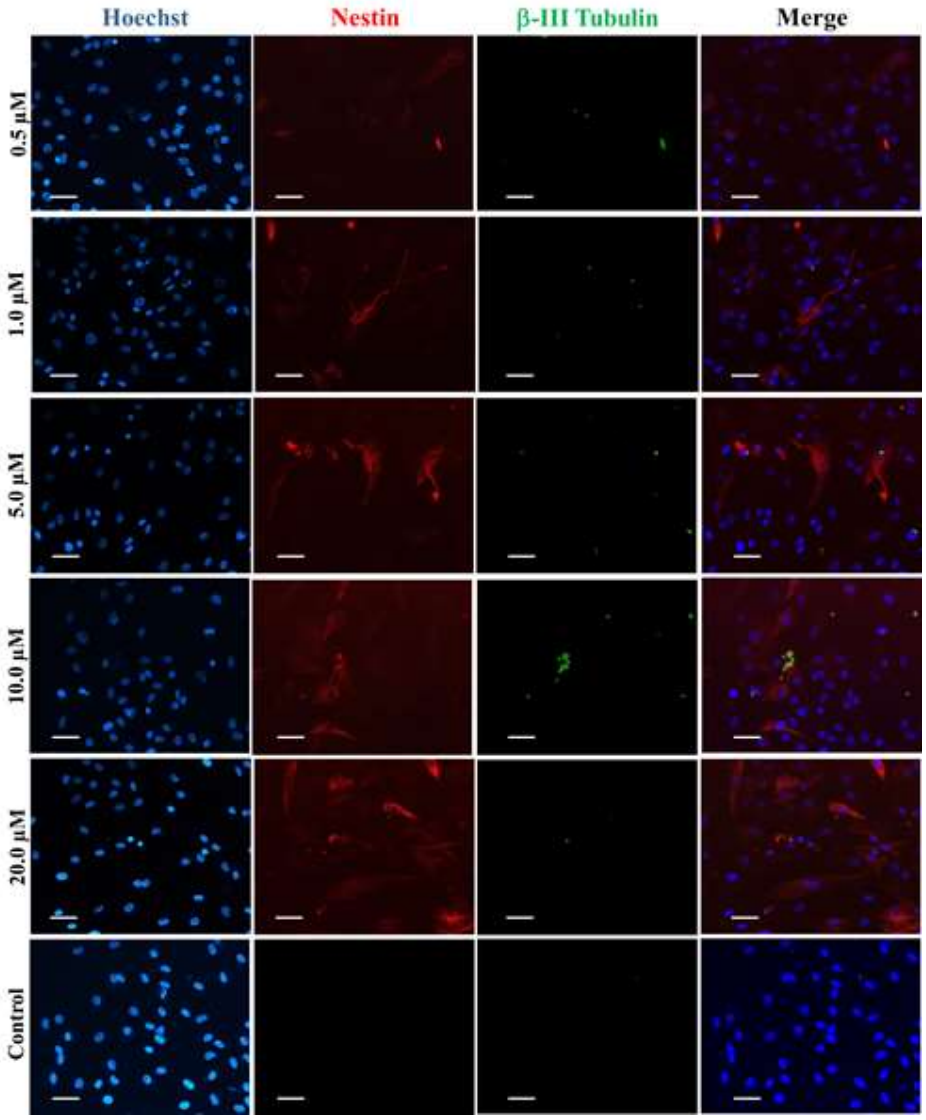

Figure 6.9: Shows an image of different staining (Hoechst, Nestin, β-III Tubulin and merge) of adherent hMSCs on ITO surface cultured in different concentrations of retinoic acid (0.5 µM, 1.0 µM, 5.0 µM, 10.0 µM, 20.0 µM and control condition (0.1% DMSO)) after day 7 of the culture.

outcomes of the proposed studies of electrostimulation to hMSCs for achieving selective differentiation into neurons. The experimental details are described in annexure I. The effect of retinoic acid on the differentiation of hMSCs towards neuronal lineage was studied and compared with the proposed approach of electrostimulating the stem cells for driving neuronal differentiation of hMSCs of cell density 1×10^4 were seeded onto ITO surface for 24

h at 37°C. Afterward, the seeded hMSCs were incubated with 20 µM, 10 µM, 5 µM, 1 µM and 0.5 µM RA in growth medium with a final DMSO concentration of 0.1% (v/v). **Figure 6.7** shows the retinoic acid stimulated hMSCs were imaged on day 1 using a fluorescence microscope and the expression of neural markers (nestin and β-III tubulin) was quantified by performing immunocytochemistry. Similarly, the response of expression of neural markers (nestin and β-III tubulin) after retinoic acid stimulated hMSCs were quantified on day 3 and day 7. Their results are shown in Figures 6.8 and **6.9**, respectively. The results showed no expression of both nestin and β-III tubulin on day 1 and day 3 even for the highest concentration of RA employed in the study. After day 7 of stimulation, the cells showed expression of only nestin and relative red fluorescence intensity increased with increased concentration of RA. These observations are similar to previously reported findings (Gao et al., 2014; George et al., 2019). This confirms the superiority of the use of the electrochemical method reported for initiating neurodifferentation within 24 h and start achieving maturation by day 3.

6.5 Neurogenic differentiation of hMSCs by electrical stimulation

After providing one cycle of stimulation at different potential biasing ranges, the adherent hMSCs were further incubated in fresh culture media. As the cell viability and proliferation, studies showed that voltage biases in the range of - 0.5 V to + 0.5 V and - 1.0 V to + 1.0 V did not have any adverse effect on the cells. Thus, these conditions were further used to investigate expression of neurogenic markers at different time points after receiving electrostimulation to the hMSCs on conducting (ITO) surface. These are described as electrostimulated (ES), and adherent hMSCs on the ITO surface without biasing (± 0.0 V) are defined as unstimulated (US). To assess the differentiation capacity of stimulated hMSCs,

different neural-specific markers, nestin, and β-III tubulin, were evaluated by immunocytochemical analysis. Nestin is an intermediate filament protein exclusively expressed in neural precursor cells, while β-III tubulin represents commitment towards neuron cells. The ES and US hMSC on ITO platforms were washed with PBS and fixed by incubation with 4% paraformaldehyde for 15 min at room temperature. Subsequently, blocking buffer (0.3% Triton X-100 and 5% normal goat serum in PBS) were added to these platforms for 1 h. Then these permeabilized platforms

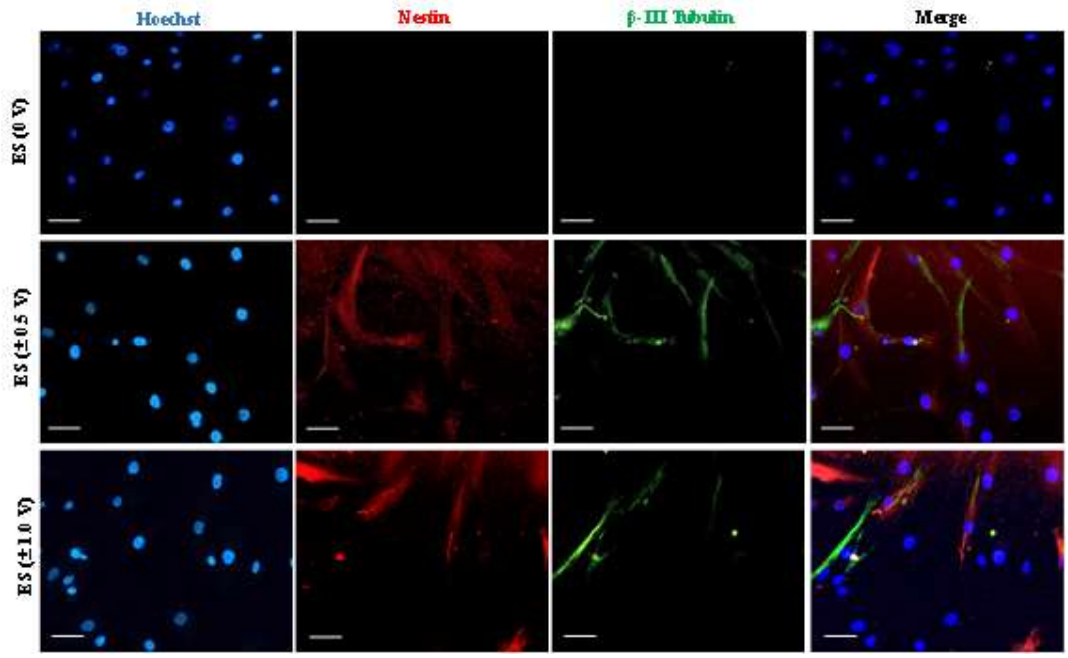

Figure 6.10: Expression of neurogenic markers. Nestin and β-III tubulin were counterstained with Hoechst 33342 for hMSCs adherent to the ITO surface with (± 0.5 V and ± 1.0 V) electrostimulation and without stimulation (ES (0 V)) on day 1 of receiving the stimulation.

were washed with PBS and incubated overnight at 4°C with anti-nestin (1:3200) and anti-β-III tubulin (1:300) overnight at 4°C. Afterward, the cells were washed with PBS and incubated with diluted secondary antibody (1:1000) for 2 h at room temperature in the dark. The cells were counterstained with Hoechst and visualized by a fluorescence microscope.

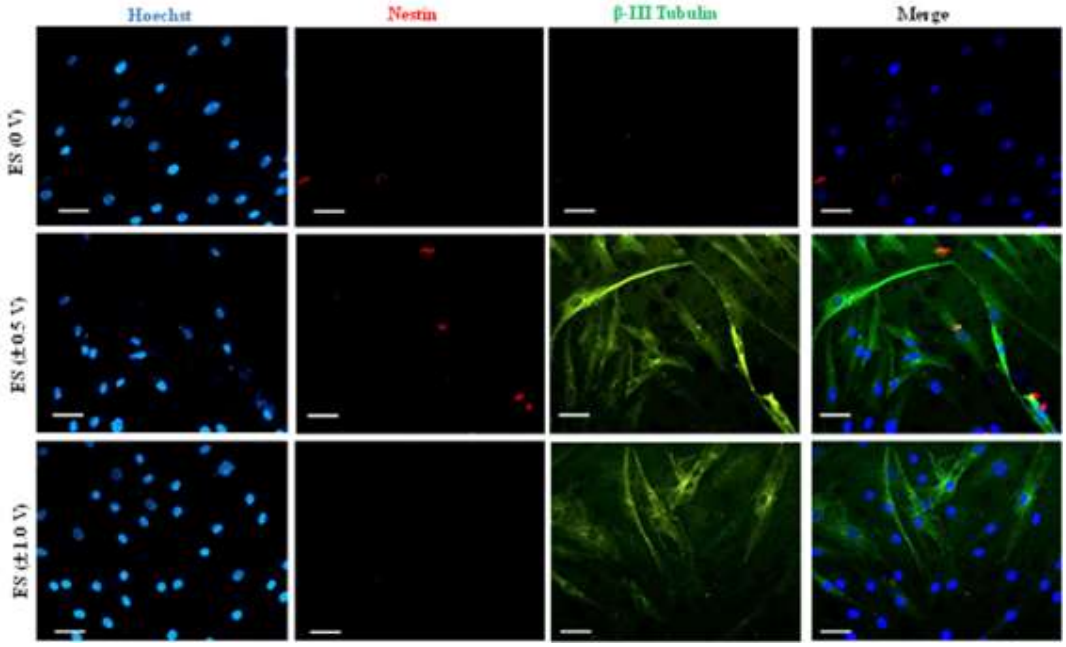

Figure 6.11: Expression of neurogenic markers. Nestin and β-III tubulin were counterstained with Hoechst 33342 for hMSCs adherent to the ITO surface with (± 0.5 V and ± 1.0 V) electrostimulation and without stimulation (ES (0 V)) on day 3 of receiving the stimulation.

Their differentiation state was assessed by staining for neurogenic cell surface markers (nestin and β-III tubulin) by immunocytochemistry. Time-dependent assessment of these markers was imaged by staining different cell surface markers and results after day 1, day 3 and day 7 or receiving electrostimulation are shown in **Figure 6.10**, **Figure 6.11**, and **Figure 6.12**, respectively. The finding reveled after examination of assessment of these markers that the nestin expression were initiated just after 24 h of electrostimulation. With further progression of the time, these decreases were observed on day 3 (**Figure 6.11**) and day 7 (**Figure 6.11**).

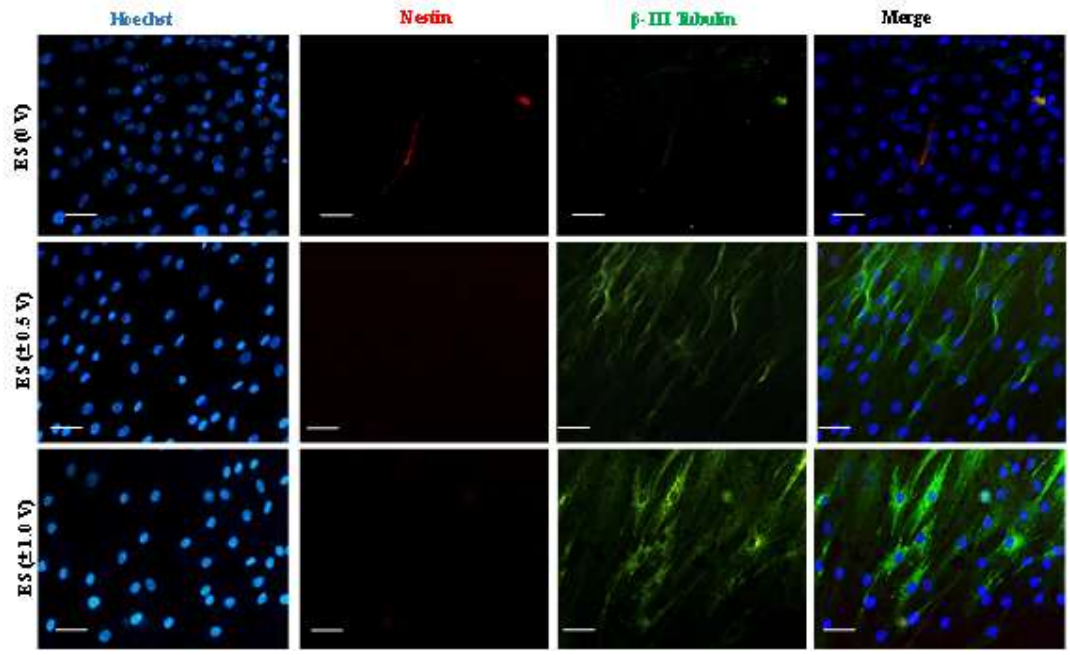

Figure 6.12: Expression of neurogenic markers. Nestin and β-III tubulin were counterstained with Hoechst 33342 for hMSCs adherent to the ITO surface with (± 0.5 V and ± 1.0 V) electrostimulation and without stimulation (ES (0 V)) on day 7 of receiving the stimulation.

The expression of β-III tubulin commencement at day 3 in the study, indicated neural progenitors' commitment to form neurons. Another interesting correlation can be drawn that the expression of nestin begins much early and then the expression of β-III tubulin, thus initially the conversion of hMSC into neural progenitors' commitment and then transforming towards further maturation into neurons. The qualitative analysis from microscopic images shows that there was not much difference in the level of expression of the neuronal marker in the hMSCs received electrostimulation at biasing of -1.0 V to + 1.0 V and – 0.5 V to + 0.5 V. The cells grown at control conditions (known as without stimulation) on conducting surface showed no expression of neurogenic cell surface markers (nestin and β-III tubulin) obtained by immunocytochemistry. Further, analysis at day 7 showed an increased expression level of β-III tubulin and a relative decrease in the nestin expression for the cells that received the electrostimulations.

6.6 Quantification of morphological changes in hMSCs using scanning electron microscopy

Cell surface morphology of neurons represented with unique characteristics, scanning electron microscopy (SEM) was used to image the morphology of the hMSCs before and after different days of receiving electrostimulation. For the analysis, the samples were prepared by gently washing the cells adherent platforms with PBS and fixing them in 4% paraformaldehyde solution for 15 min. Then, the solution was poured out, followed by washing and finally dehydrating them by dipping in solutions of 30%, 50%, 70%, 80%, 90%, and 100% ethanol. The prepared platforms were air-dried and imaged without gold coating. The ES hMSCs showed cell morphology resembling neural-like cells, confirmed by SEM (**Figure 6.13**). The images demonstrated that the spindle-shaped hMSCs transformed into elongated cells with outgrowths after stimulation.

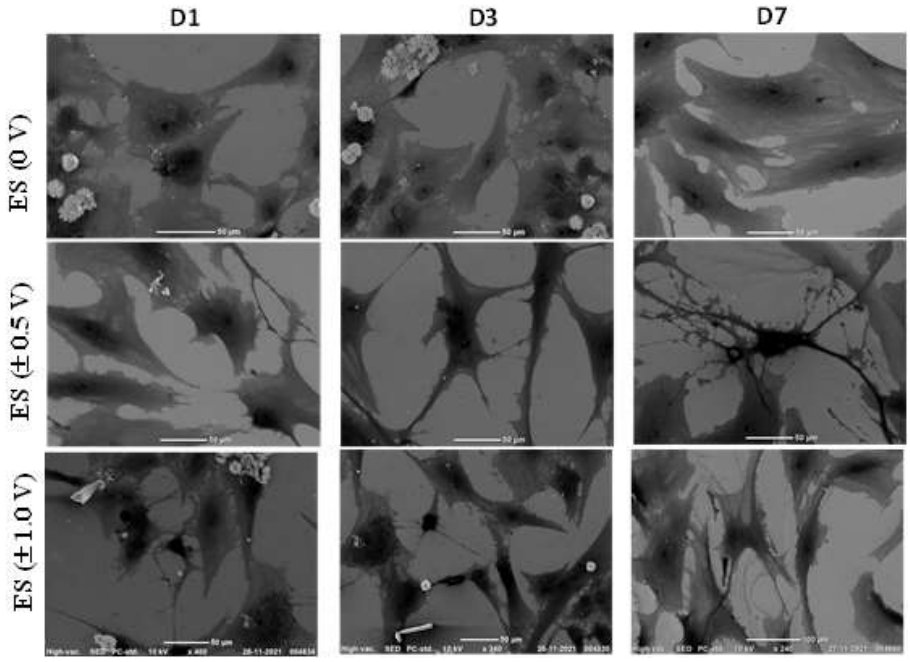

Figure 6.13: shows SEM images of cells on different days after receiving electrical stimulation under various conditions. D1 (day 1), D3 (day 3) and D7 (day 7).

6.7 Assessment of mitochondrial membrane potential

The mechanism for the differentiation of hMSCs through electrostimulation has been investigated by quantifying the mitochondrial membrane potential (MMP, $\Delta\Psi_M$). The mitochondrial membrane potential (MMP), $\Delta\Psi_M$, was assessed using the lipophilic fluorescent probe, JC-1, which accumulates within mitochondria depending on their $\Delta\Psi_M$. The dye exhibits a monomeric form and emits a green fluorescence intensity when MMP is low (depolarization). In contrast, mitochondria with high MMP (hyperpolarization) fluoresce red signal due to aggregates formation. $\Delta\Psi_M$ was measured as fluorescence emission in cells that received stimulation and cells that did not.

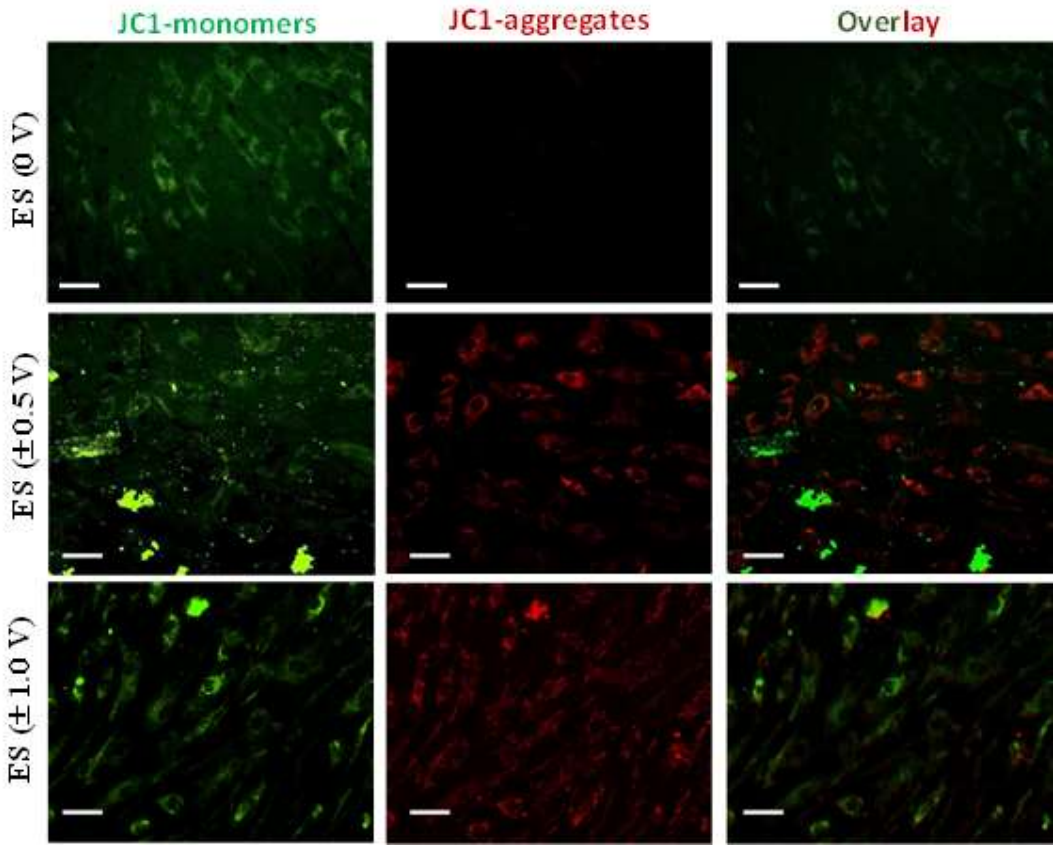

Figure 6.14: Expression of mitochondrial membrane potential associated with JC-1 monomers and aggregates for hMSCs adherent to the ITO surface that received different stimulations (± 0.5 V and ± 1.0 V) on the day 1 after it received stimulation. ES (0 V) corresponds to hMSCs without receiving electrical stimulation. The scale bar is 10 μM.

The stimulated and unstimulated hMSCs laden platforms at specified days (D1, D3, and D7) were washed once with cold PBS and stained with JC-1 dye (2 μM) for 20 min in dark at 37°C in a CO_2 incubator. The supernatant was aspirated and cells were washed twice with PBS and examined immediately. Images were acquired using a Nikon Eclipse 90i fluorescence microscope. Time-dependent assessment of these markers was imaged by staining and results after day 1, day 3 and day 7 or receiving electrostimulation are shown in **Figure 6.14**, **Figure 6.15**, and **Figure 6.16**, respectively.

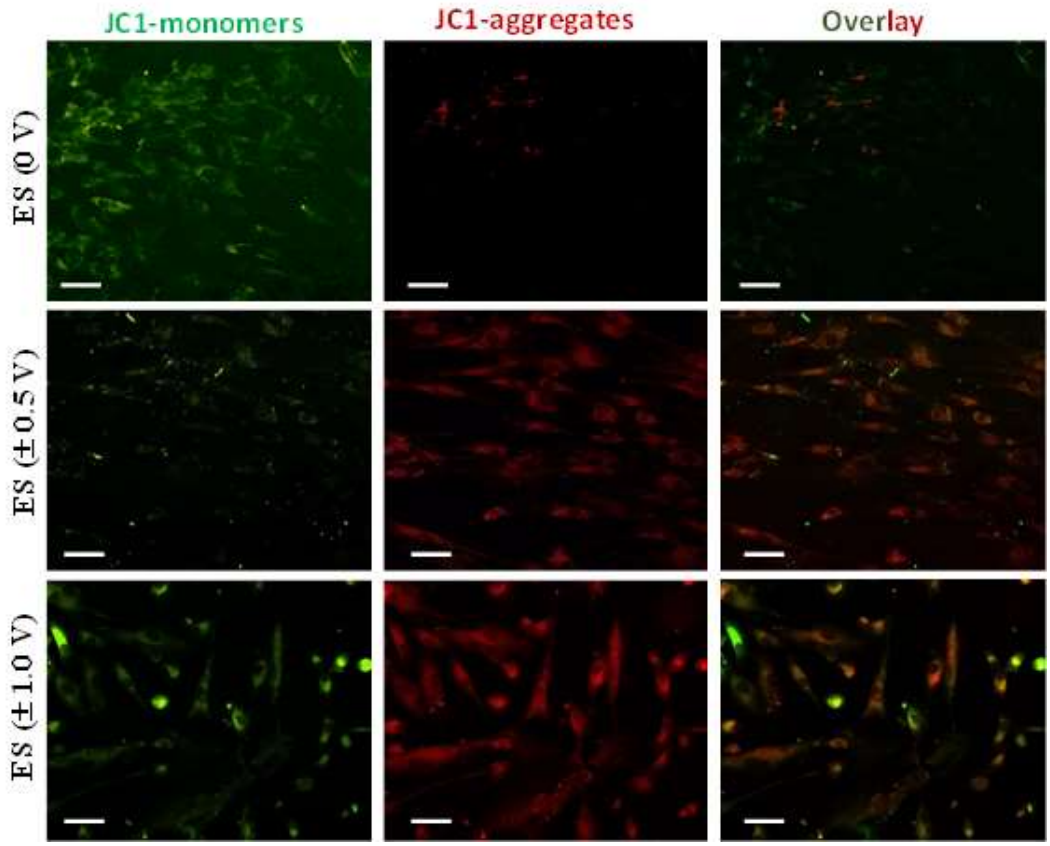

Figure 6.15: Expression of mitochondrial membrane potential associated with JC-1 monomers and aggregates for hMSCs adherent to the ITO surface that received different stimulations (± 0.5 V and ± 1.0 V) on the day 3 after it received stimulation. ES (0 V) corresponds to hMSCs without receiving electrical stimulation. The scale bar is 10 μM.

It is hypothesized that electrical stimulation hyperpolarizes the mitochondrial membrane, ameliorating the proton (H^+) influx in its intermembrane space. During this process, electrons flow through mitochondrial electron transport chain (mETC) enzymatic complexes [295]. However, some electrons leak mainly from complexes I, II, or III and interact with molecular oxygen to form superoxide (O^{2-}) in the mitochondrial matrix [296]. Therefore, mitochondrial membrane potential (MMP), $\Delta\Psi_M$, a crucial central intermediate between cellular energy supply and energy demand in oxidative energy metabolism, was assessed to unravel the changes within mitochondria during the differentiation process [297,298]. Mitochondrial polarization was monitored by staining cells (ES and US) with JC-1 at different time points.

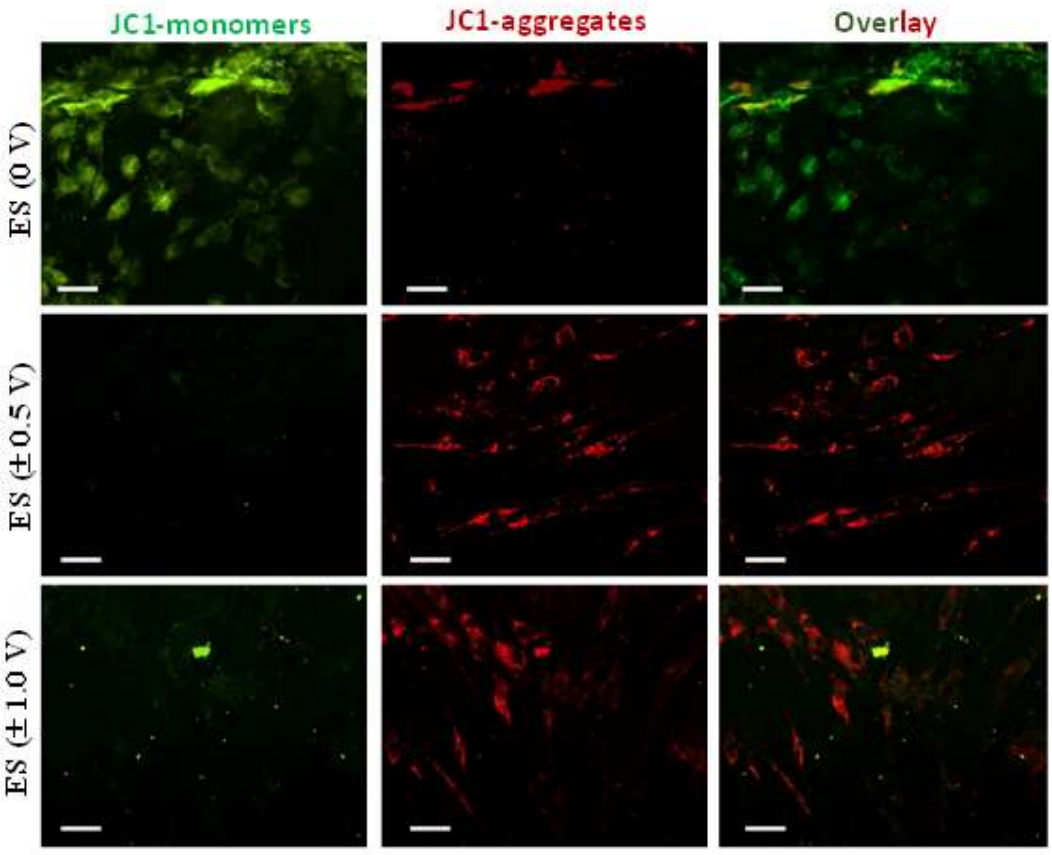

Figure 6.16: Expression of mitochondrial membrane potential associated with JC-1 monomers and aggregates for hMSCs adherent to the ITO surface that received different stimulations (± 0.5 V and ± 1.0 V) on the day 7 after it received stimulation. ES (0 V) corresponds to hMSCs without receiving electrical stimulation. The scale bar is 10 μM.

With the progression of time after stimulation, a rise in MMP was observed in the ES hMSCs, confirmed by the red fluorescent signal of JC-1 aggregates (**Figures 6.14**, **6.15**, and **6.16**). The finding indicated the mitochondria become polarized as hMSCs transform towards neuronal lineage.

6.8 Estimation of intracellular reactive oxygen species (ROS)

The effect of increased MMP on intracellular reactive oxygen species (ROS) generation was evaluated using the fluorescent dye, DCFH-DA. In the experiment, DCFH-DA dye was employed to monitor the changes in levels of intracellular ROS in stimulated hMSCs compared to the unstimulated population. Briefly, DCFH-DA, a cell-permeant dye, is deacetylated to a non-fluorescent compound by cellular esterases and further oxidized to form a green fluorescent 2'-7'dichlorofluorescein (DCF) product in the presence of ROS.

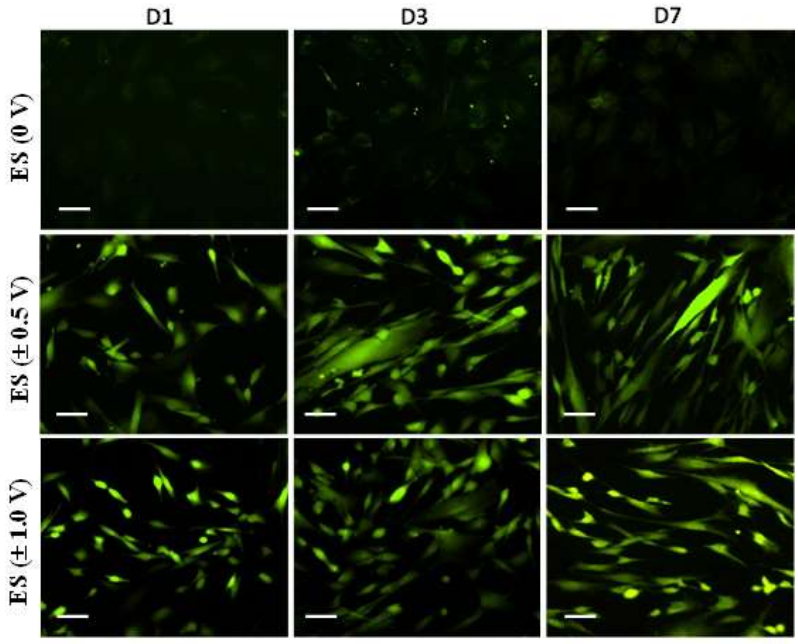

Figure 6.17: Expression of ROS in hMSCs adherent to the ITO surface that received different stimulations (± 0.5 V and ± 1.0 V) at different days after it received stimulation. ES (0 V) corresponds to hMSCs without receiving electrical stimulation. Day 1 (D1), day 3 (D3) and day 7 (D7). The scale bar is 10 μM.

After the incubation period, the hMSCs adherent on ITO platforms were washed with cold PBS twice and loaded with 10 µM DCFH-DA (in PBS) for 30 min at 37°C in the dark. After the incubation, the cells were washed to remove the unbound dye. Fluorescence images were captured using an inverted fluorescence microscope. Three independent experiments were performed for ROS estimation on days 1, 3 and 7 after stimulation. The quantitative assessment of DCF green fluorescence signal was done using Image J software (n= 10). In electrostimulated cells, an augmentation in intracellular reactive oxygen species (ROS) generation (**Figure 6.17**). ROS generation in cells is tightly associated with the oxidative phosphorylation pathway of cellular respiration, acting as a key messenger to induce neuronal differentiation [299-305].

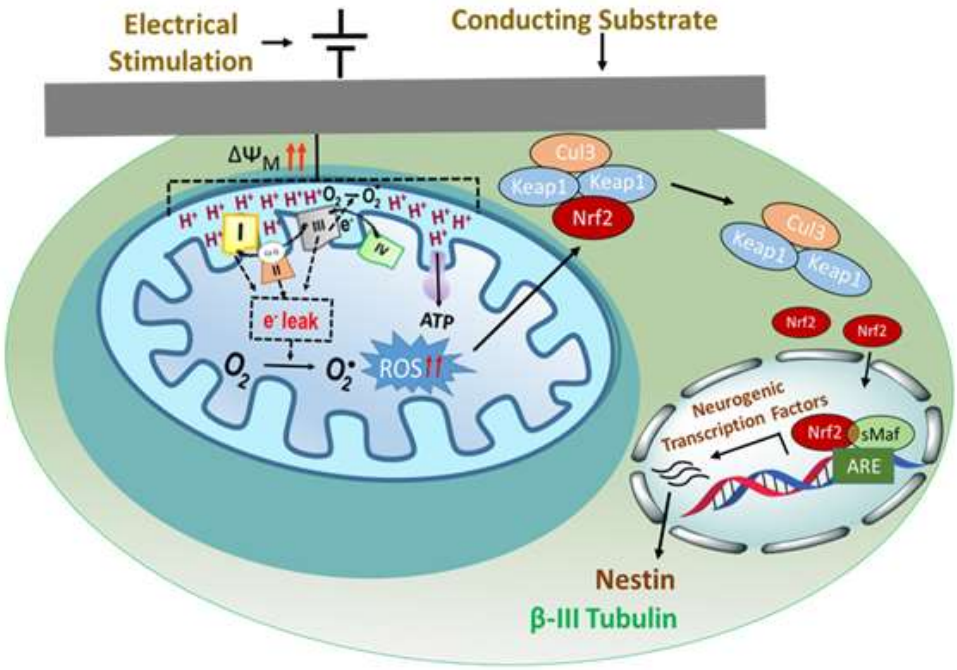

Figure 6.18: Schematic representation of the effect of electrical stimulation causing hyperpolarization of mitochondrial membrane potential and protonation of intermembrane space leading to electron leakage from different complexes and their participation in the generation of ROS. The excess production of ROS cleves off Nrf2, leading to the activation of neurogenic transcription factors.

In contrast, the US hMSCs showed a low fluorescence ratio of JC-1 red aggregates to green monomers with no production of ROS, thereby retaining their original characteristics. A possible mechanism to explain is proposed in the schematic diagram in **Figure 6.18**. This described the hyperpolarization of MMP, leading to excess ROS production and hence activation of neurogenic transfections factors [306-309].

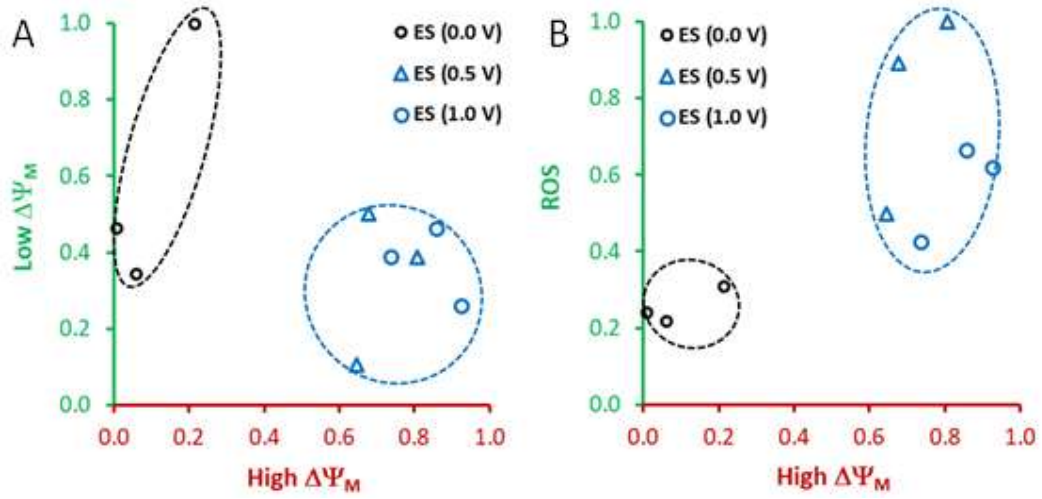

Figure 6.19: (A) A plot of low ΔΨM and high ΔΨM, indicates two distinct regions for unstimulated hMSCs (black) and stimulated hMSCs leading to neurogenic differentiation (blue). (B) A plot of ROS and high ΔΨM, indicates two distinct regions for unstimulated hMSCs (black) and stimulated hMSCs leading to neurogenic differentiation (blue). The fluorescence intensity of the signal was measured using Image J software (n= 10).

6.9 Mechanism for electrochemical differentiation of hMSC: Correlation of MMP and ROS

The reported finding above has advanced our understanding in finding the relationship between mitochondrial bioenergetics adjudicating ROS generation and stem cell differentiation. It was further hypothesized that enhanced ROS participates in the dissociation of nuclear factor-erythroid factor 2-related factor 2 (Nrf2) from its repressor protein complex,

Kelch-like ECH-associated protein 1 (KEAP1) and cullin-3 (Cul3) into the cytoplasm [310-312]. Free Nrf2 dimerizes with small musculoaponeurotic fibrosarcoma (MAF) proteins and binds together to the antioxidant response element (ARE) region of DNA, which leads to the activation of neural-specific transcription factors [313,314] as illustrated in schematic **Figure 6.19**. Our studies demonstrated that during the differentiation process, the $\Delta\Psi_M$ transition from low to high values was quantitatively assessed by measuring the fluorescence intensity of JC-1 monomers and their aggregate formation. **Figure 6.19A** shows the relative change between low $\Delta\Psi_M$ and high $\Delta\Psi_M$, indicating two distinct regions representing the population of US and ES hMSCs. This change in $\Delta\Psi_M$ indicated hyperpolarization of the mitochondrial membrane due to electrostimulation. Quantitative assessment of ROS with high $\Delta\Psi_M$ was examined for ES and US hMSCs. Interestingly, we observed a positive correlation between ROS production and high $\Delta\Psi_M$ during neurogenic differentiation (**Figure 6.19B**). En masse, we deduced that electric stimulation resulted in hyperpolarizing the mitochondrial potential, which enhanced the rate of ROS emission by mETC, thereby inducing neurogenic differentiation. This was in line with previous findings, which reported a relationship between MMP and ROS [306-309]. These observations illustrate that the magnitude of MMP can be a crucial determinant in defining stem cell fate.